Computational Biology and Chemistry 111 (2024) 108112

Contents lists available at ScienceDirect

Computational Biology and Chemistry

journal homepage: www.elsevier.com/locate/cbac

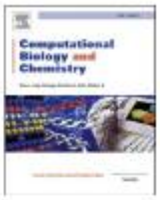

Computational therapeutic repurposing of tavaborole targeting arginase-1 for venous leg ulcer

Naveen Kumar V, T. Tamilanban *

Department of Pharmacology, SRM College of Pharmacy, SRM Institute of Science and Technology, Kattankulathur, Chengalpattu, Tamil Nadu - 603 203, India

ARTICLE INFO

Keywords:
Venous leg ulcer
Docking
Dynamics
Tavaborole
Arginase
Drug-repurposing

ABSTRACT

Venous leg ulcers (VLUs) pose a growing healthcare challenge due to aging, obesity, and sedentary lifestyles. Despite various treatments available, addressing the complex nature of VLUs remains difficult. In this context, this study investigates repurposing boronated drugs to inhibit arginase 1 activity for VLU treatment. The molecular docking study conducted by Schrodinger GLIDE targeted the binuclear manganese cluster of arginase 1 enzyme (2PHO). Further, the ligand-protein complex was subjected to molecular dynamic studies at 500 ns in Gromacs-2019.4. Trajectory analysis was performed using the GROMACS simulation package of protein RMSD, RMSF, RG, SASA, and H-Bond. The docking study revealed intriguing results where the tavaborole showed a better docking score (-3.957 Kcal/mol) compared to the substrate L-arginine (-3.379 Kcal/mol) and standard L-norvaline (-3.141 Kcal/mol). Tavaborole interaction with aspartic acid ultimately suggests that the drug molecule binds to the catalytic site of arginase 1, potentially influencing the enzyme's function. The dynamics study revealed the compounds' stability and compactness of the protein throughout the simulation. The RMSD, RMSF, SASA, RG, inter and intra H-bond, PCA, FEL, and MMBSA studies affirmed the ligand-protein and protein complex flexibility, compactness, binding energy, van der waals energy, and solvation dynamics. These results revealed the stability and the interaction of the ligand with the catalytic site of arginase 1 enzyme, triggering the study towards the VLU treatment.

1. Introduction

Venous leg ulcers (VLUs) are wounds of insidious onset with a prolonged history; currently, they are the most common form of wound in elderly populations and are increasing, with predicted escalation in relation to such variables as obesity and sedentary lifestyle (Mayrovitz et al., 2023). This augmented part presents an obligation to carry extra financial pressure on the healthcare systems for appropriate treatment plan. Venous valve dysfunction causes venous reflux, which is a characteristic of chronic venous insufficiency (CVI) and predisposes people to VLUs. Primary reasons, such as valve incompetence, interrupt normal blood flow; while secondary factors, such as worsen congestion, obesity, and impede microcirculation, that add to VLU development (Atkin and Clothier, 2023). VLUs develop from the complex sequence of events, including reflux and hypertension due to CVI, which lead to tissue injury and ischemia. Dysregulated inflammation, driven by cytokines and growth hormones, enhances tissue damage and delayed healing, worsened by matrix metalloproteinases (MMPs) (Raffetto and Khalil, 2021). It is crucial for the healthcare professionals treating VLU to understand this pathway. The exudate from the venous leg ulcer varies from serous and serosanguinous to purulent, depending on the current inflammation status and the infection's level and state. VLUs are linked to cellulitis infection and soft tissue by the bacteria clinging to the wounds. These conditions have a close affinity with the species of *Staphylococcus aureus*, *Streptococcus* organisms, and *Pseudomonas aeruginosa* (Ong et al., 2022; Sari and Suryawati, 2023). Besides, deep vein thrombosis (DVT) may occur in cases connected to venous leg ulcers due to the increased risk of blood clotting in deep veins. Chronicity and ulcer recurrences of VLUs are the factors that cause the most trouble for patients and the healthcare system in particular.

VLUs treatment can be based on multiple drugs that help the cicatrization by different mechanisms. Topical agents such as silver sulfadiazine are aimed at their antimicrobial properties, thus providing a moist environment that can serve as a protective/preventive or treatment against infections (Norman et al., 2018). Systemic drugs like pentoxifylline increase blood circulation and help reduce inflammation. They improve the process of healing (Sun et al., 2021). Biologics like becaplermin gel, containing recombinant human platelet-derived

* Correspondence to: Department of Pharmacology, SRM College of Pharmacy, SRM Institute of Science and Technology, Kattankulathur 603203, India.
E-mail address: tamilant@srmist.edu.in (T. Tamilanban).

https://doi.org/10.1016/j.compbiolchem.2024.108112
Received 9 April 2024; Received in revised form 21 May 2024; Accepted 23 May 2024
Available online 27 May 2024

growth factor (PDGF), elicits cell proliferation and collagen synthesis, which aid in wound closure (Goldman, 2004). Pain management is accomplished by medications like ibuprofen, which are non-steroidal anti-inflammatory drugs (NSAIDs) that alleviate discomfort by reducing swelling (Purcell et al., 2020). Infection control is vital and it is partly achieved by using antibiotics like cephalexin (Keflex) to prevent pathogen proliferation (O'Meara et al., 2014). Supportive care like hyperbaric oxygen therapy (HBOT) can increase tissue oxygenation and angiogenesis, further facilitating wound healing (Lalieu et al., 2021). Despite progress in wound care, the best therapeutic strategies for venous ulcers are yet to be developed, further highlighting the urgent need for novel therapeutic options. Factors such as venous pathogenesis, delayed wound healing, and patient-related factors accumulate as causes of chronic VLU, and CVI is foremost among them. The recurrence rates vary from 50% to 70% in the first 5 years and are usually associated with unresolved venous problems and inadequate treatment (Raffetto et al., 2020).

Among many targets, the urea cycle enzyme arginase 1 has become a viable target for VLU because of its regulatory function in immunological responses and metabolic pathways. Research reveals that the activity of arginase 1 affects the equilibrium between activities that promote inflammation and healing, which in turn affects the course of wound healing (Drago et al., 2016; Szondi et al., 2021). Key residues for targeting inhibition of arginase 1 activity will usually include those with coordination with the metal ions in the active site and the residue of great importance for the binding of the substrate and its role in catalysis. Specifically, the manganese ions are the prime targets. The metal ions in the active site substrate contain catalytic residues and aspartic acid (ASP128 and ASP183), which coordinates with the metal ions and histidine (HIE126). In addition, a tyrosine residue exists at the active site that functions in substrate binding and catalysis (Di Costanzo et al., 2007). Normally, arginase 1 inhibitors target these critical residues in an enzyme as one way of interfering with the function of an enzyme. In this regard, inhibitors that can bond the residues could, therefore, disrupt the mechanisms either of the substrate binding or the catalytic mechanism itself, hence inhibiting, effectively, the enzyme from carrying out its activity.

Boronated drugs (drugs containing boron atoms in their molecule) open up new ways of therapeutic exploration. The element boron can be a remarkable extent, bind with biological macromolecules and subcellular to cellular functions in general, and, therefore, promises attractive possibilities for alternative selective therapy (Nzietchueng et al., 2002; Demirci, 2015). Besides, the contribution of boron in determining both inflammatory responses and metabolic pathways runs with the objective of routine wound healing. The repurposing of an FDA-approved boronated drug for use in targeting Arginase 1 is a tantalizing possibility in venous ulcer therapy. Leveraging current safety and pharmacokinetic data simplifies medication development and aligns with drug repurposing concepts. This research intends to propose an alternative treatment strategy for venous ulcers, addressing their multifactorial character by examining the possibility of repurposing a boronated drug to inhibit arginase 1 activity using in-silico docking and molecular dynamic investigations.

2. Materials and methods

2.1. Molecular docking

Molecular docking studies are used to determine the binding affinity of ligand-protein binding. For molecular docking studies, the Glide module of Schrodinger v12 was utilized to accurately assess the potential interactions between the crystal structure of human arginase I enzyme (PDB ID: 2PHO) with L-arginine (substrate), L-norvaline (standard) and tavaborole (drug). Glide has the least errors of less than 1 Å and is recognized to be more accurate at locating the right poses of docked ligand complexes (Friesner et al., 2004).

2.1.1. Preparation of ligands

The SDF file of L-arginine, L-norvaline, and tavaborole was downloaded from PubChem, and its energy minimization was done. The structures were optimized using the OPLS_2005 force field to yield one low-energy 3D structure with the correct chirality and docking preparedness. The Schrodinger LigPrep module and Chemsketch, both part of Schrodinger Maestro 9.3, were the tools utilized for this. The LigPrep module ensures the ligand has the right amount of protons added for a desired docking with the targets under research (Bhandare et al., 2022; Lokhande et al., 2022).

2.1.2. Preparation of receptor protein

The structure of arginase 1 protein was retrieved from the Protein Data Bank (PDB) website (https://www.rcsb.org). Typically, protein X-ray crystallographic structures available in PDB format contain cofactors, heavy atoms, and water molecules. Prior to docking simulations, these structures require processing. To prepare the protein structures for docking simulations, Schrödinger's Protein Preparation Wizard was employed to optimize the structures for use with Glide and ensure chemical accuracy.

Binding site prediction of the selected targets was conducted using Schrödinger, employing a rigid receptor model. The Glide program utilizes hierarchical filters to facilitate an accurate match between ligand and receptor for successful docking with the Emodel. The resulting validated protein structures from molecular docking were then analyzed to investigate the interactions between the protein and ligands, specifically 2PHO with substrate, standard, and drug (Di Costanzo et al., 2007).

2.2. Molecular dynamics

The crystal structure of human arginase I complexed with thiosemicarbazide at 1.95 Å resolution (2PHO). The selected top ligands identified from docking analysis include L-arginine (2PHO-DRG), tavaborole (2PHO-SUB), and L-norvaline (2PHO-STD). Ligand topology was selected from the ATB server. The pdb2gmx, a module of GROMACS, was used to add hydrogens to the heavy atoms. Prepared systems were the first vacuum minimized for 1500 steps using the steepest descent algorithm. Then, the structures were solvated in a cubic periodic box with a water simple point charge (SPCE) water model. The complex systems were subsequently maintained with an appropriate salt concentration of 0.15 M by adding suitable Na and Cl counter ions. The system preparation was referred to based on a previously published paper by Gangadharappa et al. (2020). Each resultant structure from the NPT equilibration phase was subjected to a final production run in the NPT ensemble for 500 ns simulation time. Finally, the trajectory of the simulation was analyzed using various tools provided by the Gromacs software package, including the protein root mean square deviation (RMSD), root mean square fluctuation (RMSF), radius of gyration (RG), solvent accessible surface area (SASA), hydrogen bonding (H-Bond). The molecular Mechanics Poisson-Boltzmann surface area (MM-PBSA) approach was employed to understand the binding free energy (2PHO-SUB and 2PHO-STD binding) of an inhibitor with protein over simulation time. A GROMACS utility g_mmpbsa was used to estimate the binding free energy (Kumari et al., 2014). To ensure precise outcomes, we computed 2PHO-SUB and 2PHO-STD for different windows, for 2PHO-DRG (310–400 ns and 470–500 ns), 2PHO-SUB (270–350 ns and 460–500 ns) and 2PHO-STD (240–270 ns, 295–325 ns and 410–480 ns) with dt 1000 frames.

Principal Component Analysis (PCA) was employed to explore the collective movements within the protein complexes. PCA is a dimensionality reduction technique that identifies the principal modes of motion within a system. By analyzing the first few eigenvectors (EVs), which represent the major modes of motion, the conformational dynamics of the protein complexes were examined throughout the simulation. The time evolution of PCA was utilized to assess the overall

flexibility of the complexes. Lower overall flexibility observed on both EVs indicated stability within the complexes.

Free Energy Landscapes (FELs) were generated to further investigate protein folding methods and general stability. FEL maps provide insights into the most stable conformational ensembles of a protein structure by mapping energy levels across different conformational states. For PC1 and PC2, FEL plots were generated, where deeper blue areas with lower energy and greater stability indicate favorable protein conformations.

3. Results

3.1. Molecular docking

Molecular docking studies were conducted to investigate the binding interactions of various compounds with the active site of human arginase 1 (PDB ID: 2PHO) to inhibit its activity. Three compounds, L-arginine, L-norvaline, and tavaborole, were selected for analysis. The Glide scores obtained for the compounds ranged from -3.957 kcal/mol to -3.141 kcal/mol, indicating favorable binding interactions with the enzyme (Table 1). Among the compounds tested, tavaborole exhibited the highest Glide score (-3.957 kcal/mol), followed by L-arginine (-3.379 kcal/mol) and L-norvaline (-3.141 kcal/mol). Similarly, Glide energy values ranged from -22.177 kcal/mol to -15.688 kcal/mol, with L-norvaline demonstrating the lowest Glide energy (-15.688 kcal/mol). Analysis of the amino acid residues involved in the binding interactions revealed distinct binding patterns for each compound. For L-arginine, interactions were observed with ASN130, ASP183, and GLU186 residues (Fig. 1). L-norvaline interacted with MN614, MN615, THR246, and HIE126 residues (Fig. 2). Tavaborole demonstrated interactions with ASP128 residue (Fig. 3).

3.2. Molecular dynamics

3.2.1. Root Mean Square Deviation (RMSD)

The RMSD values were examined over time to learn more about the behavior of the systems and to look into the stability of the protein-ligand complex (Fig. 4). Based on the simulation findings; it can be concluded that both systems achieved equilibrium in less than 50 ns and maintained an equal distribution throughout. Additionally, by analyzing the RMSD values, it was determined that the docked complex remained stable for up to 100 ns for the 2PHO-APO, 2PHO-DRG, 2PHO-SUB, and 2PHO-STD. The average RMSD values for 2PHO-APO, 2PHO-DRG, 2PHO-SUB and 2PHO-STD were determined to be 0.23 +/- 0.03 nm, 0.25 +/- 0.03 nm, 0.21 +/- 0.02 nm and 0.22 +/- 0.03 nm, respectively. This finding suggests that the 2PHO-DRG, 2PHO-SUB, and 2PHO-STD are stable systems that did not exhibit significant fluctuations during the simulation.

3.2.2. Root Mean Square Fluctuation (RMSF)

RMSF is utilized in MD simulations to quantify the variations of each residue and flexible area of a protein. It is possible to ascertain the effect of ligand binding on the protein by examining RMSF during simulations. In general, RMSF values are greater in loosely organized loop regions and lower in compact protein structures like helices and sheets. In this investigation, the RMSF values were computed and displayed for every residue in 2PHO-APO, 2PHO-DRG, 2PHO-SUB, and 2PHO-STD complexes (Fig. 5). The average RMSF values for 2PHO-APO, 2PHO-DRG, 2PHO-SUB and 2PHO-STD were determined to be 0.16 +/- 0.1 nm, 0.16 +/- 0.1 nm, 0.12 +/- 0.1 nm and 0.17 +/- 0.2 nm, respectively. The results indicate that the 2PHO-APO, 2PHO-DRG, 2PHO-SUB, and 2PHO-STD complex did not significantly alter the overall RMSF distribution.

Table 1
Molecular docking score of compounds targeting arginase 1.

S. No	Compound Name	Ligand	Glide score (Kcal/mol)	Glide energy (Kcal/mol)
1	L-arginine	Substrate	-3.379	-16.729
2	L-norvaline	Standard	-3.141	-15.688
3	Tavaborole	Drug	-3.957	-22.177

3.2.3. Radius of gyration (Rg)

To assess the dynamic stability and compactness of 2PHO, its 2PHO-DRG, 2PHO-SUB, and 2PHO-STD complex, the Rg values were computed and graphed (Fig. 6). The average Rg values for 2PHO-APO, 2PHO-DRG, 2PHO-SUB and 2PHO-STD were determined to be 1.93 +/- 0.03 nm, 1.86 +/- 0.02 nm and 1.86 +/- 0.01 nm, respectively. The complex system of 2PHO-DRG exhibited almost similar Rg values compared to the 2PHO-SUB and 2PHO-STD complex system, indicating a similar compactness of both complex systems.

3.2.4. Solvent accessible surface area (SASA)

SASA is a vital metric for assessing a protein molecule's accessibility in a solvent environment. In this investigation, the SASA values were computed and displayed to examine the influence of 2PHO-DRG, 2PHO-SUB, and 2PHO-STD binding on the target's solvent accessibility (Fig. 7). The plot reveals a similar pattern in the SASA values of 2PHO-DRG, 2PHO-SUB, and 2PHO-STD. The average SASA values for 2PHO-APO, 2PHO-DRG, 2PHO-SUB and 2PHO-STD were determined to be 148.85 +/- 3.76 nm, 145.38 +/- 4.01 nm and 141.36 +/- 3.63 nm, respectively. The SASA values show fair equilibration without significant fluctuations throughout the simulation.

3.2.5. Intra and inter hydrogen bond

To assess the stability of protein (2PHO-APO) and protein-ligand (2PHO-DRG, 2PHO-SUB, and 2PHO-STD complex) interactions, the formation of Intra and Inter Hydrogen Bonds plays a crucial role. In this study, we investigated the time-dependent behavior of intra-hydrogen bonds 2PHO-APO, 2PHO-DRG, 2PHO-SUB, and 2PHO-STD complexes and plotted the results (Fig. 8). The average intra H-Bond values for 2PHO-APO, 2PHO-DRG, 2PHO-SUB, and 2PHO-STD Complex were determined to be 215.22 +/- 8.7 nm, 221.29 +/- 8.0 nm, 214.89 +/- 8.04 nm and 220 +/- 8.16 nm, respectively. The plot revealed that higher hydrogen bonds being formed in the 2PHO-DRG, 2PHO-SUB, and 2PHO-STD complex than in the 2PHO-APO form of the protein; the result indicated that 2PHO-DRG, 2PHO-SUB, and 2PHO-STD complex had more stability compared to the 2PHO-APO form.

Establishing hydrogen bonds is critical in determining the stability of protein-ligand interactions. In this work, we evaluated the time-dependent behavior of inter molecular hydrogen bonding between 2PHO-DRG, 2PHO-SUB, and 2PHO-STD and displayed the findings (Fig. 9). Based on the findings, a minimum of one to three hydrogen bonds with the 2PHO-DRG complex, and one to five hydrogen bonds with the 2PHO-SUB and 2PHO-STD complex kept the docked complex stable throughout the simulation.

3.2.6. Principal Component Analysis (PCA)

To explore the collective movements in 2PHO-APO, 2PHO-DRG, 2PHO-SUB, and 2PHO-STD, we conducted PCA. A protein molecule's overall motion is greatly influenced by its first few eigenvectors (EVs). Therefore, throughout the simulation, we used PCA to examine the conformational dynamics of 2PHO-APO and 2PHO-DRG, as well as 2PHO-SUB and 2PHO-STD (Fig. 10). The 2PHO-APO, 2PHO-DRG, 2PHO-SUB, and 2PHO-STD complexes showed lower overall flexibility on both EVs, according to the time evolution of PCA, indicating stability. The Fig. 10 makes it abundantly evident that the complexes of 2PHO-APO, 2PHO-DRG, 2PHO-SUB, and 2PHO-STD occupied almost all conformational movements and overlapped. As a whole, the reduced number of movements seen in the 2PHO-DRG, 2PHO-SUB, and 2PHO-STD shows that 2PHO-DRG, 2PHO-SUB, and 2PHO-STD did not substantially impact the target conformation and dynamics, therefore confirming the stability of the complex.

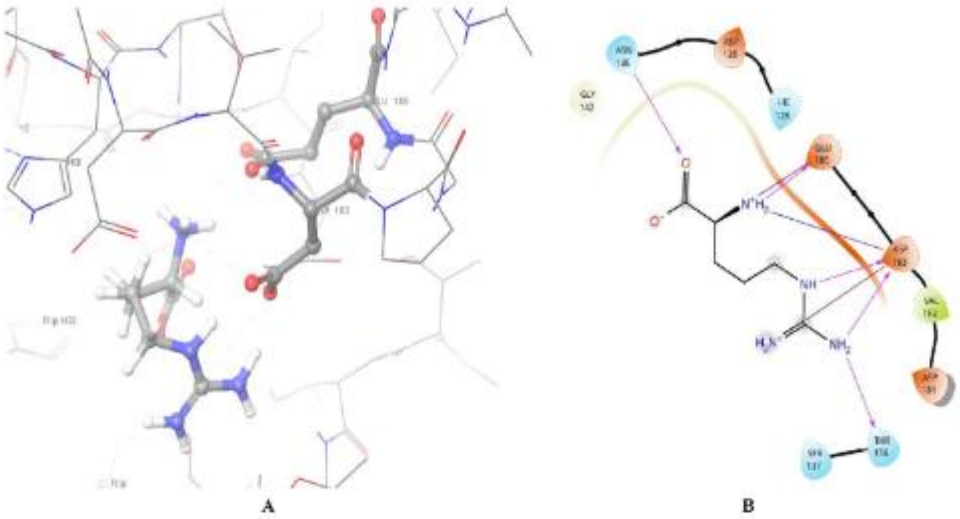

Fig. 1. Interaction of L-arginine with the active domain of the arginase 1 enzyme. (A) 3D interaction; (B) 2D interaction.

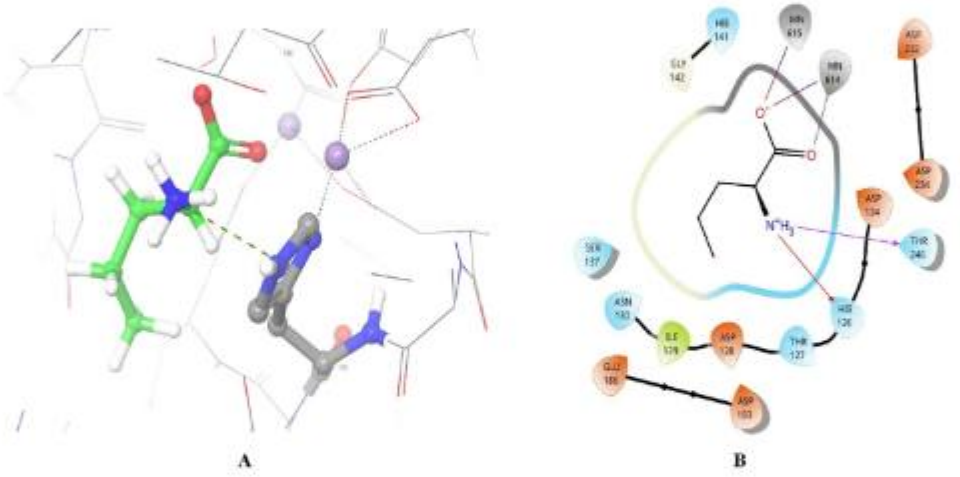

Fig. 2. Interaction of L-norvaline with the active domain of the arginase 1 enzyme. (A) 3D interaction; (B) 2D interaction.

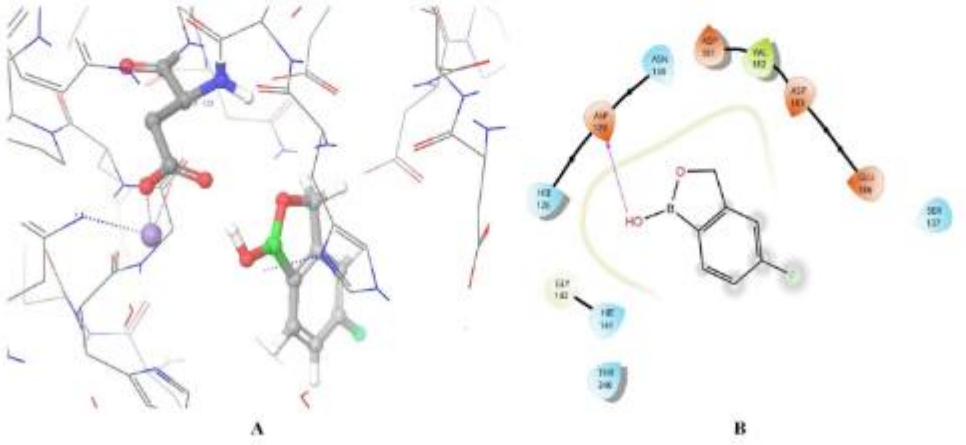

Fig. 3. Interaction of tavaborole with the active domain of the arginase 1 enzyme. (A) 3D interaction; (B) 2D interaction.

3.2.7. Free Energy Landscapes (FELs)

One common tool for examining protein folding methods and general stability is the examination of free energy landscapes, or FELs. For a given protein structure, FEL maps show which conformational ensembles are the most stable. For PC1 and PC2, FEL plots were generated (Fig. 11), whereby deeper blue areas with lower energy and greater stability are indicative of a protein conformation. The Fig. 11 depict energy levels ranging from 0 to 16 kJ/mol during the simulation

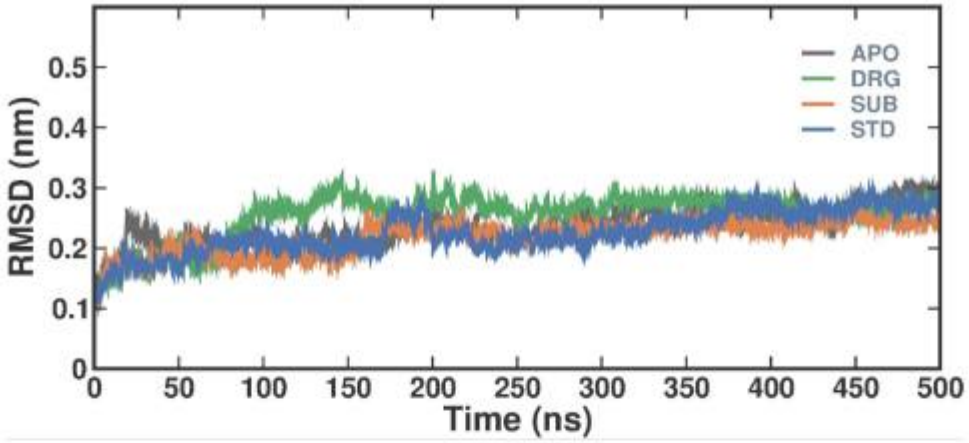

Fig. 4. RMSD Conformational dynamics analysis of 2PHO-APO, 2PHO-DRG, 2PHO-SUB, and 2PHO-STD.

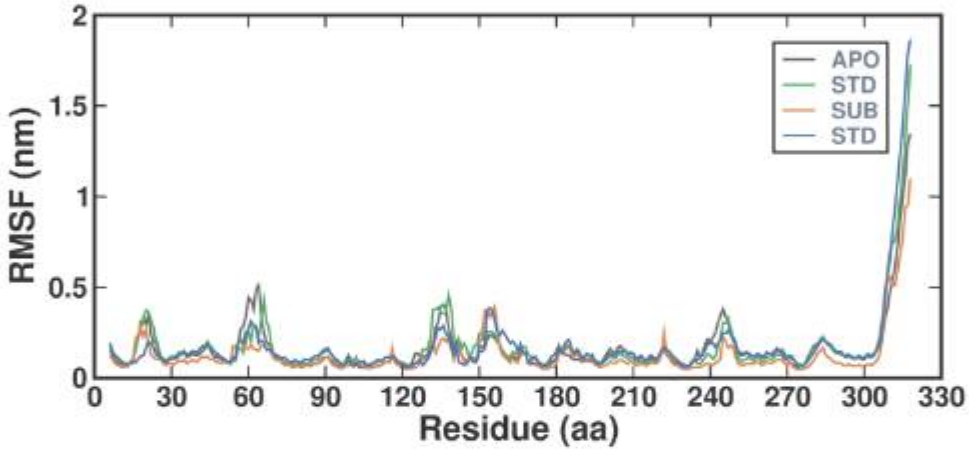

Fig. 5. RMSF Conformational dynamics analysis of 2PHO-APO, 2PHO-DRG, 2PHO-SUB, and 2PHO-STD complex.

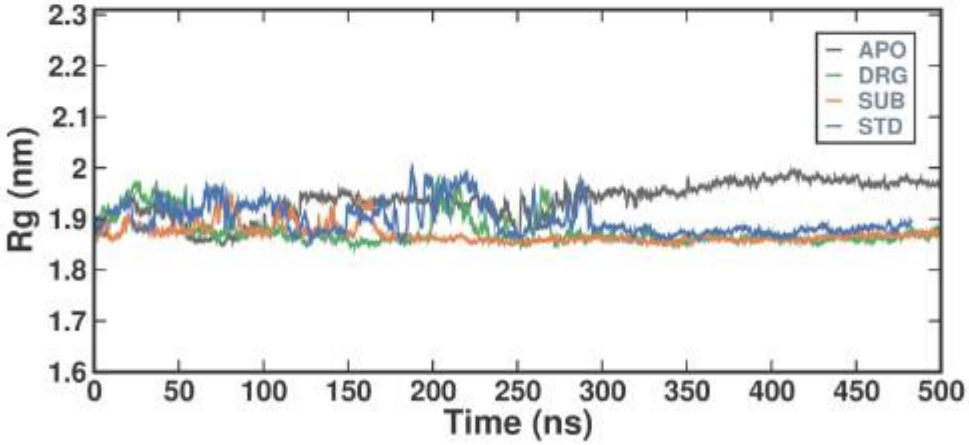

Fig. 6. Rg Conformational dynamics analysis of 2PHO-APO, 2PHO-DRG, 2PHO-SUB, and 2PHO-STD complexes.

of 2PHO-APO and 0–20 kJ/mol throughout the simulation of 2PHO-DRG, 2PHO-SUB, and 2PHO-STD, respectively. The FEL plots demonstrate that the 2PHO-DRG, 2PHO-SUB, and 2PHO-STD complex have a single global minimum, restricted to a broad local basin. These results show that 2PHO-DRG, 2PHO-SUB, and 2PHO-STD do not produce any major conformational changes in the target structure, therefore stabilizing it (Fig. 11).

3.2.8. MM - PBSA

The relative binding strength inside the protein of summery energy was investigated in order to ascertain the binding affinities of 2PHO-DRG, 2PHO-SUB, and 2PHO-STD. Table 2 presents a comparison of the binding strengths of 2PHO-DRG, 2PHO-SUB, and 2PHO-STD with respect to inhibitors, as calculated using the MM-PBSA approach. Across a steady simulation trajectory, we determine residue-level contributions to the interaction energy.

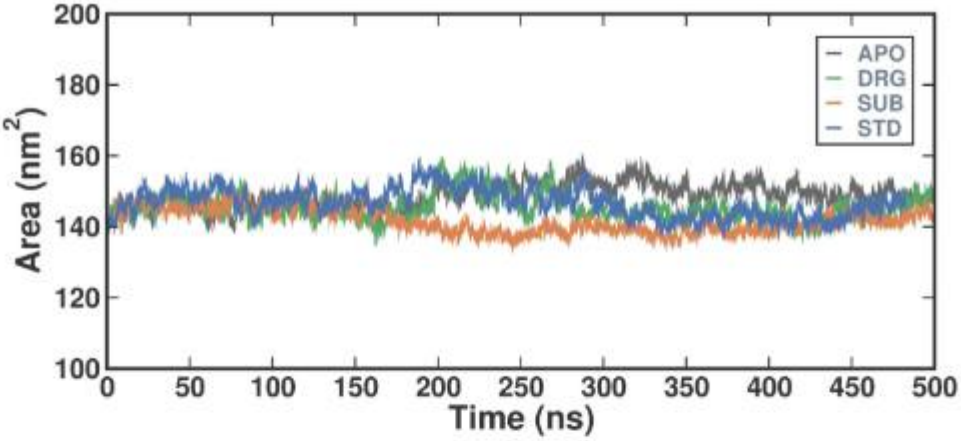

Fig. 7. SASA Conformational dynamics analysis of 2PHO-APO, 2PHO-DRG, 2PHO-SUB, and 2PHO-STD complexes.

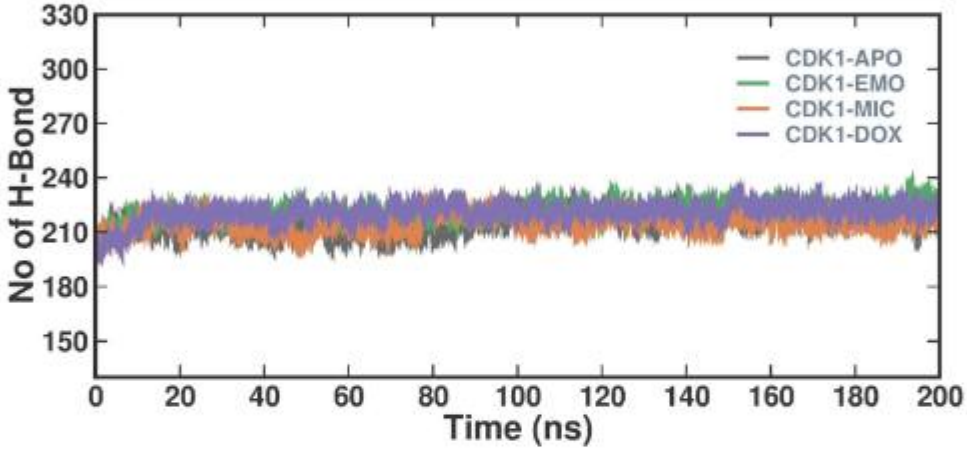

Fig. 8. Intramolecular hydrogen bonds 2PHO-APO, 2PHO-DRG, 2PHO-SUB, and 2PHO-STD during the simulation time.

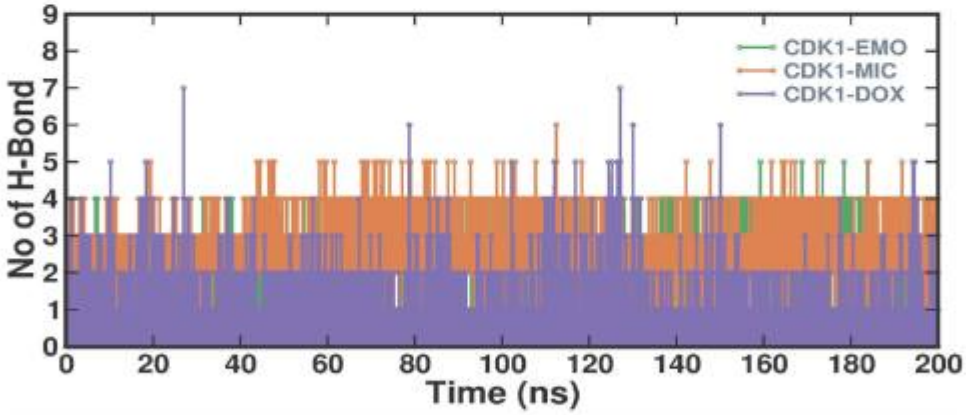

Fig. 9. Intermolecular hydrogen bonds between protein-ligand during the simulation time.

The MM-PBSA results provide insights into the energetics of the studied systems. The 2PHO-DRG system observed relatively stable van der Waals and electrostatic energies, suggesting consistent non-covalent interactions between the drug and its target. However, notable fluctuations in polar solvation and binding energies indicate solvent molecules' influence and the binding interface's dynamic nature. The 2PHO-SUB system, in contrast, displayed huge variability in all the energy terms. The strongly negative electrostatic energy can be said to denote very strong Coulombic forces between the substrate and arginase 1. In contrast, the large range for the polar solvation energies might indicate differences in the extent of stabilization that is caused by the solvent mediation. The fluctuation of the binding energy may indicate the dynamic nature of the substrate-arginase interaction, probably comprising conformational changes and reorganization of the solvent. The 2PHO-STD system showed rather stable van der Waals energies, indicating relatively consistent contacts of a non-covalent nature. Instead, the electrostatic and polar solvation energies point out their sensitivity regarding the solvent environment and likely variability of the charge

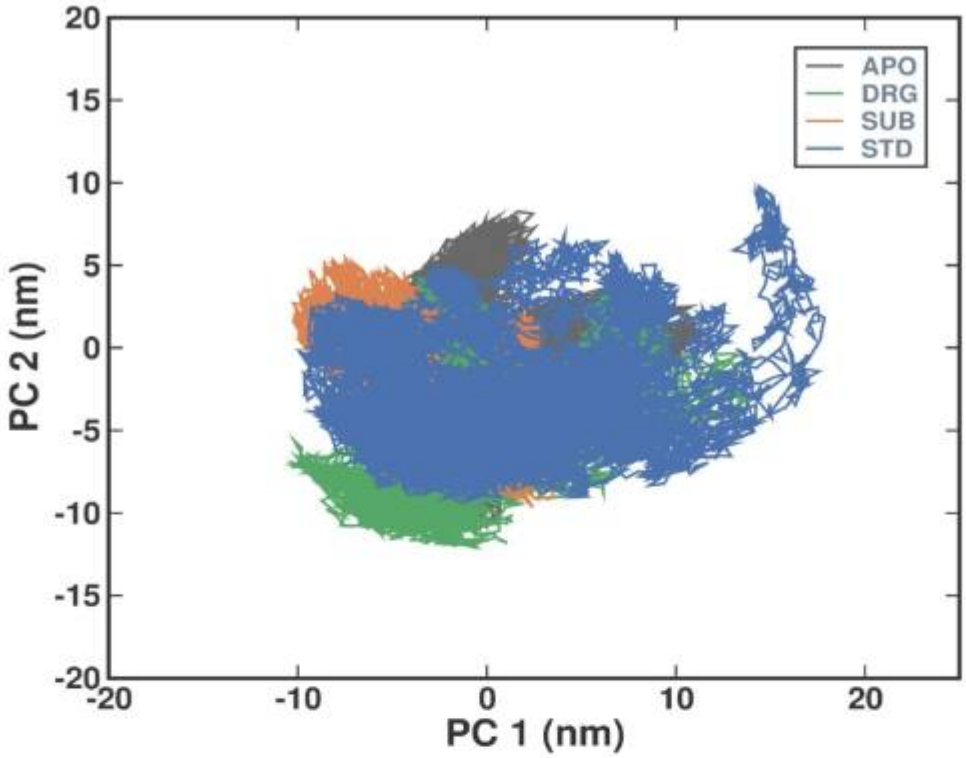

Fig. 10. Principal component analysis 2D projection plot shows the conformation sampling of 2PHO-APO, 2PHO-DRG, 2PHO-SUB, and 2PHO-STD on PC1 and PC2.

distribution. The results regarding the binding energies are hence strongly varied, indicating the strong complexity of the standard molecule's interaction with the environment, solvent dynamics, and conformational flexibility.

4. Discussion

In this study, we investigated the arginase 1 inhibition potential of FDA-approved boronated drugs through molecular docking and dynamics studies, with a focus on identifying a suitable candidate for topical application in venous leg ulcers. Our selection criteria focused on a drug with good pharmacological properties and the least possible adverse reactions when applied topically. Among the candidate boronated drugs, tavaborole looks very promising and was found to be further considered. The first is the fact that bortezomib, Delanzomib, and ixazomib are already known to be associated with skin adverse reactions and, therefore, not good for application topically in venous leg ulcers (Marah et al., 2023; Vogl et al., 2017). Vaborbactam was also rejected for this, although it is a beta-lactamase inhibitor, due to differences in pharmacological properties. Crisaborole, even with the potential to serve as an arginase inhibitor, was not selected because, in some reports, it has led to an increase in arginase activity. In contrast, tavaborole, as a marketed topical solution, was an attractive drug. On the one hand, the established safety profile of tavaborole (Mahajan et al., 2024; Yousefian et al., 2024) and its mode of action as a leucyl-tRNA synthetase inhibitor provide confidence in the potential repurposing of this compound in the context of arginase 1 inhibition (Zhang and Ma, 2019). The favorable docking results, characterized by a strong Glide score and Glide energy, suggest a robust binding affinity between tavaborole and the active site residue ASP128. This interaction is pivotal due to the central role of ASP128 in the catalytic mechanism of arginase 1. In-depth analysis reveals that ASP128 likely plays a crucial role in coordinating metal ions within the active site, contributing to the enzyme's catalytic activity. Tavaborole's interaction with ASP128 may disrupt these coordination bonds, inhibiting the enzyme's ability to bind its substrate or effectively carry out the catalytic reaction. The OH group in tavaborole can form hydrogen bonds with the side chain of ASP128 in arginase 1. Hydrogen bonding occurs when a hydrogen atom is covalently bonded to an electronegative atom, such as the oxygen atom in the carboxyl group of aspartate (Grabowski, 2011). This interaction is typically strong and directional, contributing significantly to the stability of the ligand-enzyme complex. In a recent study by Pham et al. (2016), the cinnamide derivatives were evaluated as mammalian arginase inhibitors. It was reported that chlorogenic acid showed interaction with HIS126, HIS101, ASP232, ASP124, and ASP128, while caffeic acid phenylamide (CAPA) showed interaction with HIS126, ASP232, ASP234, ASP124, and ASP128. It was established that CAPA could penetrate the catalytic site of the arginase 1 by chelating the manganese ion cofactor and interacting with the aspartic acid. A similar interaction was observed with the arginase 1 enzyme and ZINC000252286875 molecule, as reported by Zaki et al. (2023). It was identified that the ZINC000252286875 showed interaction with the ASP128 residue through amino and OH groups, and the proton uptake may be the key switch in modulating the arginase 1 function. These reported results follow the results obtained from the tavaborole interaction with the catalytic site of arginase 1, which suggests that tavaborole may disrupt the function of the arginase 1 enzyme.

In this study, MD simulations were performed to investigate the dynamic changes that occur upon binding of the target protein. Several parameters, such as RMSD, RMSF, Rg, SASA, and inter-hydrogen bonding, were calculated for both the protein and protein-ligand complex. The RMSD value of 0.21 +/- 0.03 indicates that the 2PHO-SUB complex exhibits relatively low structural deviation from the initial conformation during the simulation. On the other hand, the high RMSD value of 0.25 ± 0.03 nm for the 2PHO-DRG may be due to the dynamic nature of the enzyme-ligand interactions, mainly due to the presence of tavaborole in the active site of arginase 1. The RMSD plot for 2PHO complexes with tavaborole, L-arginine, and L-norvaline reveals stable interactions with catalytic residues, indicating sustained favorable environments throughout the simulation for all three ligands. RMSF

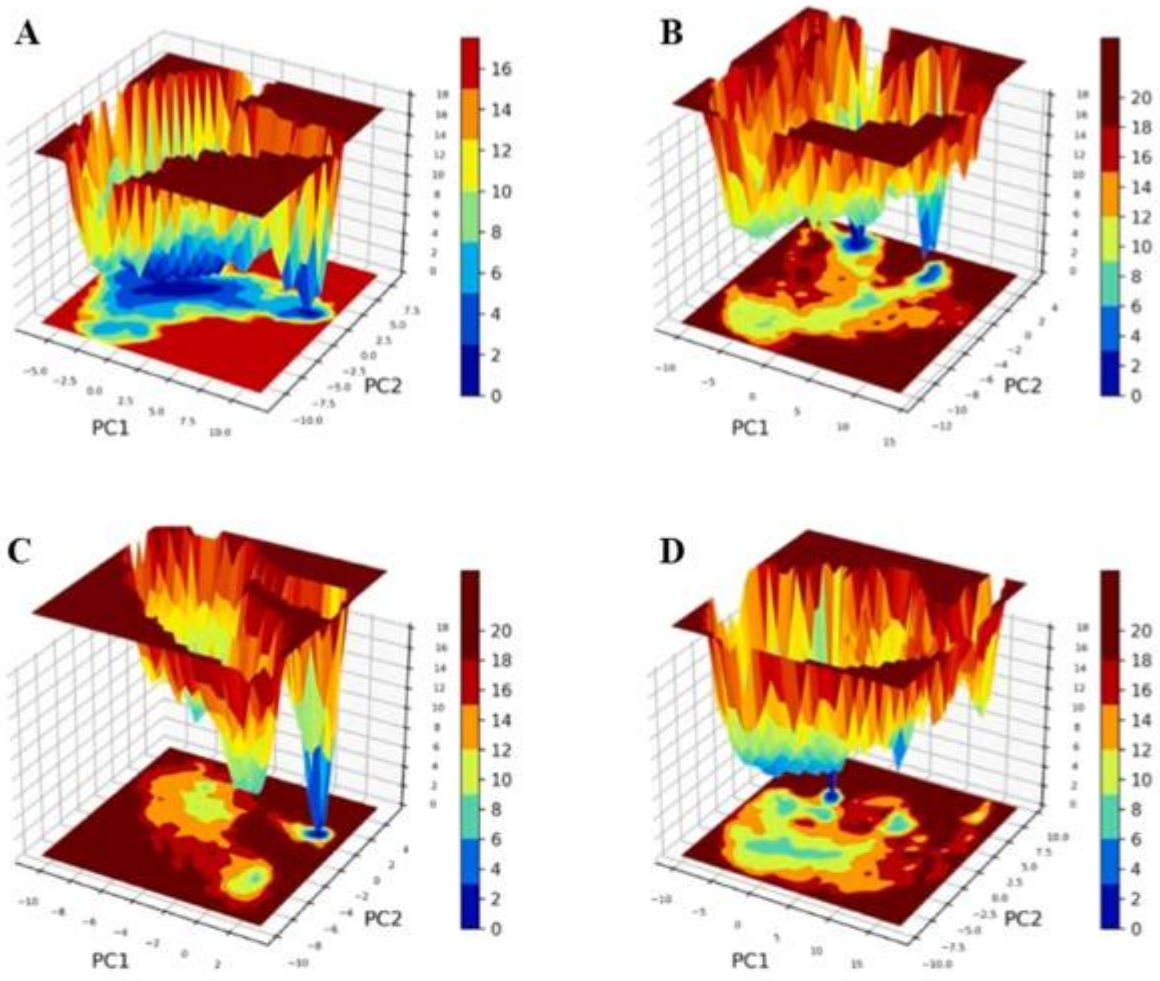

Fig. 11. The free energy landscape plots for (A) 2PHO-APO, (B)2PHO-DRG, (C) 2PHO-SUB, and (D) 2PHO-STD.

Table 2
Energy summary of the ligand-protein complex by MMPBSA.

System	Window	Van der Waal energy	Electrostatic energy	Polar solvation energy	Binding energy
2PHO-DRG-MN-H2O-R2	310–400 ns	-27.383 +/- 24.229 kJ/mol	-8.190 +/- 13.530 kJ/mol	26.526 +/- 47.286 kJ/mol	-13.234 +/- 35.236 kJ/mol
2PHO-DRG-MN-H2O-R2	470–500 ns	-26.969 +/- 25.408 kJ/mol	-2.789 +/-5.184 kJ/mol	21.404 +/- 31.781 kJ/mol	-12.088 +/- 12.542 kJ/mol
2PHO-SUB-MN-H2O	270–350 ns	-37.651 +/- 15.007 kJ/mol	-117.255 +/- 47.057 kJ/mol	173.627 +/- 42.817 kJ/mol	10.422 +/- 23.616 kJ/mol
2PHO-SUB-MN-H2O	460–500 ns	-16.650 +/- 15.640 kJ/mol	-429.079 +/- 81.559 kJ/mol	405.377 +/- 86.376 kJ/mol	-47.842 +/-7.406 kJ/mol
2PHO-STD-MN-H2O	240–270 ns	-10.461 +/- 16.436 kJ/mol	-23.269 +/- 37.739 kJ/mol	42.199 +/- 69.914 kJ/mol	6.596 +/- 42.106 kJ/mol
2PHO-STD-MN-H2O	295–325 ns	-1.374 +/-4.862 kJ/mol	-22.287 +/- 26.358 kJ/mol	56.463 +/- 16.868 kJ/mol	31.366 +/- 33.840 kJ/mol
2PHO-STD-MN-H2O	410–460 ns	-0.819 +/-1.024 kJ/mol	0.220 +/-6.704 kJ/mol	-34.268 +/- 65.973 kJ/mol	-34.695 +/- 70.966 kJ/mol

analysis was employed to assess the impact of the complexes on the flexible regions within the protein structure (Panwar and Kumar, 2021). The time-averaged analysis of the complexes revealed the fluctuations of the free and bounded proteins. The peaks observed from the plots reveal the fluctuation in the complex when the tavaborole or L-arginine or L-norvaline binds to the specific residues, especially the aspartic acid in the protein. Additionally, Rg analysis provides insight into the structural dynamics and mechanisms of folding and ligand interactions, as well as the overall flexibility of the biomolecules, hence contributing toward knowledge of processes at the atomic level (Du et al., 2016). The Rg values of 2PHO-DRG, 2PHO-SUB, and 2PHO-STD are closely related to each other, which signifies the compactness of the complex. The SASA quantifies the surface area of a molecule, which is accessible by solvent molecules, leading to insight into the surface of the molecule with respect to its hydrophobicity and hydrophilicity, and how the molecule interacts with its environment (Ausaf Ali et al., 2014). The SASA plot of the complexes has values that mean no significant fluctuations between the values. The data plotted with PCA clearly indicated that the conformational motions associated with complexes occupied a more comprehensive range of the plot, with a great deal of overlap between these complexes. It applies its eigenvectors to a collective of the movement and conformational dynamics of the protein molecules. The PCA analysis offers an almost direct assessment of the dynamic behavior of the complexes, proving stability with a suggestion of minimal perturbation by the bound ligands. Similarly, the FEL also showed no significant conformational changes in the protein.

VLUs result from complications that occur when there is sustained venous hypertension in microcirculation and damage, coupled with inflammation and other factors. Recent studies have highlighted the important role of arginase 1 (ARG1) in contributing to the persistence and delayed healing of VLUs (Szondi et al., 2021). The participation of ARG1 in the disease would offer potential therapeutic modalities and

suggest that intervention in the activity of ARG1 may open up an attractive approach for modulation. One of the main mechanisms contributing to the effect of ARG1 on VLUs is endothelial dysfunction. Endothelial dysfunction in CVI is a reduction of bioavailability of nitric oxide (NO) due to a deficiency in signaling, both in the regulation of vascular tone and its lack of producing new vessels in the pro-angiogenic wound healing processes. ARG1 competes with isomerizing eNOS for L-arginine. Increased ARG1 activity will deplete the pool of L-arginine, thus preventing the NO production capacity of eNOS and further deteriorating endothelial dysfunction (Berkowitz et al., 2003). This, in turn, further the process of venous hypertension; tissue perfusion, therefore, is worsened, and this completes the vicious circle of impaired wound healing, typical for VLUs. Furthermore, it has been suggested that ARG1 may be the pro-fibrotic factor in tissues, which is a hallmark in the setting of chronic wounds (Dias et al., 2015), as in the case of VLUs. Fibroblasts are activated due to continued inflammation and tissue injury, which causes them to deposit extracellular matrix components such as collagen. L-proline is an important downstream metabolite of the arginine metabolism by ARG1, and is, in itself, a precursor of molecules essential in collagen synthesis. In this manner, increased ARG1 activity may contribute collagen accumulation and fibrosis, and prevent proper tissue remodeling, which is a requirement for wound closure (Wang et al., 2021; Roque and Romero, 2021).

In addition to its impact on endothelium and tissue fibrosis, ARG1 also contributes to dysregulated immune responses (Huang et al., 2020) and chronic inflammation typical in VLUs. ARG1 is expressed in many immune cells, like macrophages and myeloid-derived suppressor cells (MDSCs), involved in the modulation of T-cell responses and favoring them to acquire an anti-inflammatory phenotype (Pesce et al., 2009). However, excess ARG1 activity can turn the balance toward immunosuppression, compromise the resolution of inflammation, and delay wound healing (Dixit et al., 2023). Upregulation of ARG1 in VLUs would thus most likely contribute to the immune dysregulation, that in turn could worsen the set of events already prolonging inflammation and impede switching into the reparative phase in wound healing. Next, ARG1 impacts angiogenesis through the modulation of arginine, which is a substrate for NO synthase enzymes (Wang et al., 2015). NO is a potent vasodilator and has been implicated in promoting angiogenesis. This potentially could reduce the NO formation, thus ultimately affecting angiogenesis. The reduction of angiogenesis further affects tissue ischemia in VLUs and compromises conditions concerning healing. ARG1-mediated alterations in angiogenesis may further magnify such impairment, thus setting up a vicious cycle that would be a prerequisite for the chronification of VLUs.

The repurposing of drugs offers a cost-effective and efficient avenue for discovering new therapeutic uses of existing drugs without undergoing the cumbersome, time-consuming, and costly process that it takes to develop entirely new compounds. Tavaborole, an oxaborole derivative, has been used as an antifungal drug in treating onychomycosis and this study has exhibited potent inhibitory action against arginase 1. This has far-reaching implications for VLUs because arginase 1 is now shown to be important in many of the pathological processes linked to VLU development. These findings suggest that the repurposing of tavaborole, an arginase 1 inhibitor, for VLUs provides an entirely novel therapeutic avenue that leverages the known safety profiles of existing drugs and might have the potential to be translated to the clinic more rapidly.

5. Conclusion

Repurposing tavaborole towards treating venous leg ulcer (VLU) is, therefore, one path that sure holds so much promise for the redress of what has remained a complex pathophysiology of these devastating wounds. Tavaborole with in-silico docking and dynamic studies may act on arginase 1 and provide a new junction for targeting the multiple pathological mechanisms, including endothelial dysfunction, tissue fibrosis, inflammation, immune dysregulation, and angiogenesis, associated with the development of VLUs. However, further research with clinical validation is needed to ascertain the effectiveness and safety in VLUs. Indeed, elucidating the mechanism of action of tavaborole against ARG1 allows new avenues of translating these findings into innovative therapies that will alleviate the burden of VLUs and improve the quality of life of the affected individuals.

Funding

This research/study did not receive any grant/funding.

Declaration of Competing Interest

The authors declare that they have no known competing financial interests or personal relationships that could have appeared to influence the work reported in this paper.

Acknowledgments

The authors sincerely thank Prof. V. Chitra, Dean, SRM College of Pharmacy, SRM Institute of Science and Technology, Kattankulathur, Chengalpattu, Tamil Nadu - 603 203, India and SCIOmics LLP for offering infrastructure support for conducting the simulation studies.

References

Atkin, L., Clothier, A., 2023. The role of venous intervention for the treatment of patients with venous leg ulceration. Br. J. Nurs. *32* (12), S6–S12. https://doi.org/10.12968/bjon.2023.32.12.S6.

Ausaf Ali, S., Hassan, I., Islam, A., Ahmad, F., 2014. A review of methods available to estimate solvent-accessible surface areas of soluble proteins in the folded and unfolded states. Curr. Protein Pept. Sci. *15* (5), 456–476.

Berkowitz, D.E., White, R., Li, D., Minhas, K.M., Cernetich, A., Kim, S., Burke, S., Shoukas, A.A., Nyhan, D., Champion, H.C., Hare, J.M., 2003. Arginase reciprocally regulates nitric oxide synthase activity and contributes to endothelial dysfunction in aging blood vessels. Circulation *108* (16), 2000–2006. https://doi.org/10.1161/01.CIR.0000092948.04444.C7.

Bhandare, R.R., Sigalapalli, D.K., Shaik, A.B., Canney, D.J., Blass, B.E., 2022. Selectivity profile comparison for certain γ-butyrolactone and oxazolidinone-based ligands on a sigma 2 receptor over sigma 1: a molecular docking approach. RSC Adv. *12* (31), 20096–20109. https://doi.org/10.1039/D2RA03497B.

Demirci, S., 2015. Roles and applications of boron compounds in cutaneous acute and chronic wound healing. (https://acikbilim.yok.gov.tr/handle/20.500.12812/338793).

Di Costanzo, L., Pique, M.E., Christianson, D.W., 2007. Crystal structure of human arginase I complexed with thiosemicarbazide reveals an unusual thiocarbonyl μ-sulfide ligand in the binuclear manganese cluster. J. Am. Chem. Soc. *129* (20), 6388–6389. https://doi.org/10.1021/ja071567j.

Dias, D.F., Ciambarella, B.T., Carvalho, V.D.F., Martins, M.A., 2015. Arginase 1 contributes to fibrogenesis in the lungs of silica-challenge mice, 46, PA940. https://doi.org/10.1183/13993003.congress-2015.PA940.

Dixit, R., Debnath, A., Mishra, S., Mishra, R., Bhartiya, S.K., Pratap, A., Shukla, V.K., 2023. A study of arginase expression in chronic non-healing wounds. Int. J. Low. Extrem. Wounds *22* (2), 360–368. https://doi.org/10.1177/15347346211012381.

Drago, D., Basso, V., Gaude, E., Volpe, G., Peruzzotti-Jametti, L., Bachi, A., Musco, G., Andolfo, A., Frezza, C., Mondino, A., Pluchino, S., 2016. Metabolic determinants of the immune modulatory function of neural stem cells. J. Neuroinflamm. *13* (1), 18. https://doi.org/10.1186/s12974-016-0667-7.

Du, X., Li, Y., Xia, Y.L., Ai, S.M., Liang, J., Sang, P., Ji, X.L., Liu, S.Q., 2016. Insights into protein–ligand interactions: mechanisms, models, and methods. Int. J. Mol. Sci. *17* (2), 144. https://doi.org/10.3390/ijms17020144.

Friesner, R.A., Banks, J.L., Murphy, R.B., Halgren, T.A., Klicic, J.J., Mainz, D.T., Repasky, M.P., Knoll, E.H., Shelley, M., Perry, J.K., Shaw, D.E., 2004. Glide: a new approach for rapid, accurate docking and scoring. 1. Method and assessment of docking accuracy. J. Med. Chem. *47* (7), 1739–1749. https://doi.org/10.1021/jm0306430.

Gangadharappa, B.S., Sharath, R., Revanasiddappa, P.D., Chandramohan, V., Balasubramaniam, M., Vardhineni, T.P., 2020. Structural insights of metallo-beta-lactamase revealed an effective way of inhibition of enzyme by natural inhibitors. J. Biomol. Struct. Dyn. *38* (13), 3757–3771. https://doi.org/10.1080/07391102.2019.1667265.

Goldman, R., 2004. Growth factors and chronic wound healing: past, present, and future. Adv. Ski. Wound care 17 (1), 24–35.

Grabowski, S.J., 2011. What is the covalency of hydrogen bonding? Chem. Rev. 111 (4), 2597–2625. https://doi.org/10.1021/cr800346f.

Huang, C., Wang, Y., Li, X., Ren, L., Zhao, J., Hu, Y., Zhang, L., Fan, G., Xu, J., Gu, X., Cheng, Z., 2020. Clinical features of patients infected with 2019 novel coronavirus in

Wuhan, China. lancet 395 (10223), 497–506. https://doi.org/10.1016/S0140-6736(20)30183-5.

Kumari, R., Kumar, R., Open Source Drug Discovery Consortium, Lynn, A., 2014. g_mmpbsa A GROMACS tool for high-throughput MM-PBSA calculations. J. Chem. Inf. Model. *54* (7), 1951–1962. https://doi.org/10.1021/ci500020m.

Lalieu, R.C., Akkerman, I., van Hulst, R.A., 2021. Hyperbaric oxygen therapy for venous leg ulcers: a 6 year retrospective study of results of a single center. Front. Med. *8*, 671678 https://doi.org/10.3389/fmed.2021.671678.

Lokhande, K.B., Shrivastava, A., Singh, A., 2022. Discovery of potent inhibitors against monkeypox's major structural proteins using high throughput virtual screening, large scale molecular dynamics and DFT calculations, PREPRINT (Version 1). https://doi.org/10.21203/rs.3.rs-2329229/v1.

Mahajan, K., Grover, C., Relhan, V., Jahiliani, S., Singal, A., Shenoy, M.M., Jakhar, D., Bansal, S., 2024. Nail Society of India Recommendations for Treatment of Onychomycosis in Special Population Groups. Indian Dermatol. Online J. 15 (2), 196–204. https://doi.org/10.4103/idoj.idoj_578_23.

Marah, K., Saeed, H., Mohammad, A., Munther, A., Hasan, A., 2023. Skin Rash as a Side Effect of Bortezomib: A Case Report. Cureus 15 (11). https://doi.org/10.7759/cureus.49051.

Mayrovitz, H.N., Wong, S., Mancuso, C., 2023. Venous, arterial, and neuropathic leg ulcers with emphasis on the geriatric population. Cureus *15* (4), e38123 https://doi.org/10.7759%2Fcureus.38123.

Norman, G., Westby, M.J., Rithalia, A.D., Stubbs, N., Soares, M.O., Dumville, J.C., 2018. Dressings and topical agents for treating venous leg ulcers. Cochrane Database Syst. Rev. 6 (6), CD012583 https://doi.org/10.1002%2F14651858.CD012583.pub2.

Nzietchueng, R.M., Dousset, B., Franck, P., Benderdour, M., Nabet, P., Hess, K., 2002. Mechanisms implicated in the effects of boron on wound healing. J. Trace Elem. Med. Biol. *16* (4), 239–244. https://doi.org/10.1016/S0946-672X(02)80051-7.

O'Meara, S., Al-Kurdi, D., Ologun, Y., Ovington, L.G., Martyn-St James, M., Richardson, R., 2014. Antibiotics and antiseptics for venous leg ulcers. Cochrane Database Syst. Rev. 1, CD003557. https://doi.org/10.1002/14651858.CD003557.pub5.

Ong, B.S., Dotel, R., Ngian, V.J.J., 2022. Recurrent cellulitis: who is at risk and how effective is antibiotic prophylaxis? Int. J. Gen. Med. *15*, 6561–6572 https://doi.org/10.2147%2FIJGM.S326459.

Panwar, A., Kumar, A., 2021. In-silico analysis and molecular dynamics simulations of lysozyme by GROMACS 2020.2. Ann. Rom. Soc. Cell Biol. *25* (6), 9679–9685. (https://annalsofrscb.ro/index.php/journal/article/view/7303).

Pesce, J.T., Ramalingam, T.R., Mentink-Kane, M.M., Wilson, M.S., El Kasmi, K.C., Smith, A.M., Thompson, R.W., Cheever, A.W., Murray, P.J., Wynn, T.A., 2009. Arginase-1–expressing macrophages suppress Th2 cytokine–driven inflammation and fibrosis. PLoS Pathog. *5* (4), e1000371 https://doi.org/10.1371/journal.ppat.1000371.

Pham, T.N., Bordage, S., Pudlo, M., Demougeot, C., Thai, K.M., Girard-Thernier, C., 2016. Cinnamide derivatives as mammalian arginase inhibitors: synthesis, biological evaluation and molecular docking. Int. J. Mol. Sci. *17* (10), 1656. https://doi.org/10.3390/ijms17101656.

Purcell, A., Buckley, T., King, J., Moyle, W., Marshall, A.P., 2020. Topical analgesic and local anesthetic agents for pain associated with chronic leg ulcers: a systematic review. Adv. Ski. Wound care *33* (5), 240–251. https://doi.org/10.1097/01.ASW.0000658572.14692.fb.

Raffetto, J.D., Khalil, R.A., 2021. Mechanisms of lower extremity vein dysfunction in chronic venous disease and implications in management of varicose veins. Vessel 5 (36) https://doi.org/10.20517%2F2574-1209.2021.16.

Raffetto, J.D., Ligi, D., Maniscalco, R., Khalil, R.A., Mannello, F., 2020. Why venous leg ulcers have difficulty healing: overview on pathophysiology, clinical consequences, and treatment. J. Clin. Med. *10* (1), 29. https://doi.org/10.3390/jcm10010029.

Roque, W., Romero, F., 2021. Cellular metabolomics of pulmonary fibrosis, from amino acids to lipids. Am. J. Physiol. -Cell Physiol. 320 (5), C689–C695. https://doi.org/10.1152/ajpcell.00586.2020.

Sari, L.G.M.P., Suryawati, N., 2023. Characteristics of lower extremity ulcers among patients treated at Prof. Dr. IGNG Ngoerah General Hospital, Denpasar, Bali. J. Med. Sci. (Berk. Ilmu Kedokt.) 55 (4). https://doi.org/10.19106/JMedSci005504202307.

Sun, S.Y., Li, Y., Gao, Y.Y., Ran, X.W., 2021. Efficacy and safety of pentoxifylline for venous leg ulcers: an updated meta-analysis, 15347346211050769 Int. J. Low. Extrem. Wounds. https://doi.org/10.1177/15347346211050769.

Szondi, D.C., Wong, J.K., Vardy, L.A., Cruickshank, S.M., 2021. Arginase signalling as a key player in chronic wound pathophysiology and healing. Front. Mol. Biosci. *8*, 773866 https://doi.org/10.3389/fmolb.2021.773866.

Vogl, D.T., Martin, T.G., Vij, R., Hari, P., Mikhael, J.R., Siegel, D., Wu, K.L., Delforge, M., Gasparetto, C., 2017. Phase I/II study of the novel proteasome inhibitor delanzomib (CEP-18770) for relapsed and refractory multiple myeloma. Leuk. Lymphoma 58 (8), 1872–1879. https://doi.org/10.1080/10428194.2016.1263842.

Wang, L., Bhatta, A., Toque, H.A., Rojas, M., Yao, L., Xu, Z., Patel, C., Caldwell, R.B., Caldwell, R.W., 2015. Arginase inhibition enhances angiogenesis in endothelial cells exposed to hypoxia. Microvasc. Res. *98*, 1–8. https://doi.org/10.1016/j.mvr.2014.11.002.

Wang, Y., Zhao, J., Zhang, H., Wang, C.Y., 2021. Arginine is a key player in fibroblasts during the course of IPF development. Mol. Ther. *29* (4), 1361–1363. https://doi.org/10.1016/j.ymthe.2021.02.023.

Yousefian, P., Smythe, C., Han, H., Elewski, B.E., Nestor, M., 2024. Treatment Options for Onychomycosis: Efficacy, Side Effects, Adherence, Financial Considerations, and Ethics. J. Clin. Aesthetic Dermatol. 17 (3), 24.

Zaki, M.E., Al-Hussain, S.A., Al-Mutairi, A.A., Samad, A., Ghosh, A., Chaudhari, S., Khatale, P.N., Ajmire, P., Jawarkar, R.D., 2023. In-silico studies to recognize repurposing therapeutics toward arginase-I inhibitors as a potential onco-immunomodulators. Front. Pharmacol. *14*, 1129997 https://doi.org/10.3389/fphar.2023.1129997.

Zhang, P., Ma, S., 2019. Recent development of leucyl-tRNA synthetase inhibitors as antimicrobial agents. Medchemcomm *10* (8), 1329–1341. https://doi.org/10.1039/C9MD00139E.